Breast Cancer Res Treat (2011) 129:691–701
DOI 10.1007/s10549-010-1239-7

PRECLINICAL STUDY

Local anesthetics inhibit kinesin motility and microtentacle protrusions in human epithelial and breast tumor cells

Jennifer R. Yoon · Rebecca A. Whipple · Eric M. Balzer · Edward H. Cho · Michael A. Matrone · Michelle Peckham · Stuart S. Martin

Received: 11 June 2010 / Accepted: 20 October 2010 / Published online: 11 November 2010

Abstract Detached breast tumor cells produce dynamic microtubule protrusions that promote reattachment of cells and are termed tubulin *microtentacles* (McTNs) due to their mechanistic distinctions from actin-based filopodia/invadopodia and tubulin-based cilia. McTNs are enriched with vimentin and detyrosinated α-tubulin, (Glu-tubulin). Evidence suggests that vimentin and Glu-tubulin are cross-linked by kinesin motor proteins. Using known kinesin inhibitors, Lidocaine and Tetracaine, the roles of kinesins in McTN formation and function were tested. Live-cell McTN counts, adhesion assays, immunofluorescence, and video microscopy were performed to visualize inhibitor effects on McTNs. Viability and apoptosis assays were used to confirm the non-toxicity of the inhibitors. Treatments of human non-tumorigenic mammary epithelial and breast tumor cells with Lidocaine or Tetracaine caused rapid collapse of vimentin filaments. Live-cell video microscopy demonstrated that Tetracaine reduces motility of intracellular GFP-kinesin and causes centripetal collapse of McTNs. Treatment with Tetracaine inhibited the extension of McTNs and their ability to promote tumor cell aggregation and reattachment. Lidocaine showed similar effects but to a lesser degree. Our current data support a model in which the inhibition of kinesin motor proteins by Tetracaine leads to the reductions in McTNs, and provides a novel mechanism for the ability of this anesthetic to decrease metastatic progression.

Keywords Microtentacles · Glu-tubulin · Metastasis · Kinesin · Tetracaine · Breast cancer

Electronic supplementary material The online version of this article (doi:10.1007/s10549-010-1239-7) contains supplementary material, which is available to authorized users.

J. R. Yoon · R. A. Whipple · E. M. Balzer · E. H. Cho · M. A. Matrone · S. S. Martin
Marlene and Stewart Greenebaum Cancer Center, Department of Physiology, University of Maryland School of Medicine, Baltimore, MD 21201, USA

E. M. Balzer · E. H. Cho · M. A. Matrone
Graduate Program in Life Science, Program in Molecular Medicine, Bressler Bldg, 655 W. Baltimore St., Baltimore, MD 21201, USA

M. Peckham
Institute of Molecular and Cellular Biology, University of Leeds, Leeds, UK

S. S. Martin (✉)
Bressler Bldg., Rm 10-29, 655 W. Baltimore St., Baltimore, MD 21201, USA
e-mail: ssmartin@som.umaryland.edu

Introduction

The metastatic capacity of circulating tumor cells (CTCs) to form blood-borne implantations is reduced by treatment with the amine anesthetic Tetracaine [1]. However, the specific mechanism underlying this anti-metastatic effect has not been pursued in recent years and remains incompletely understood. We have recently reported that detached breast tumor cell lines produce *microtentacles* (McTNs) that are supported by a coordination of detyrosinated α-tubulin and vimentin intermediate filaments [2, 3]. CTCs bind blood vessel walls via a cytoskeletal mechanism consistent with McTNs, and highly metastatic tumor cell lines display increased McTN frequencies [3, 4]. In this study, we investigated if the anesthetics, Lidocaine, and Tetracaine, affected the cytoskeletal structure of McTNs and their role in tumor cell reattachment.

Actin-based protrusions, such as lamellipodia and filopodia, are extensively studied for their roles in cellular migration and motility of adherent cells [5, 6]. However, the cytoskeletal dynamics after a cell is released from extracellular matrix are largely overlooked. Highly metastatic tumor cell lines circumvent anoikis, a form of apoptosis initiated by the loss of cell–matrix interactions [7, 8]. Recent observations of suspended mammary epithelial cells (MEC) and breast tumor cells indicate that cells actively develop long, dynamic microtubule-based protrusions of the plasma membrane [2]. McTNs observed in MECs and breast tumor cells of both human and murine origin facilitate efficient cell reattachment with surfaces, extracellular matrix, or during cell–cell adhesion. Compelling evidence from in vivo studies indicate the initial steps in colon carcinoma cell adhesion to hepatic microvasculature requires tubulin polymerization [4]. Inhibition of actin polymerization actually enhanced tumor cell adhesion to the hepatic microvasculature [4]. Actin depolymerizers inhibit lamellipodia, filopodia, and invadopodia, but enhances the length and frequency of McTNs[2]. The molecular mechanisms supporting McTNs are, therefore, consistent with the mechanisms that promote the reattachment of CTCs to blood vessel walls in vivo and implicate McTNs in the initial steps of tumor cell extravasation [2].

Further studies have also revealed that McTNs are specifically enriched in detyrosinated α-tubulin (Glu-tubulin), where post-translational removal of the c-terminal tyrosine exposes a glutamic acid residue. Glu-tubulin is a clinical marker of poor prognosis in breast cancer patients, but the mechanism by which tubulin detyrosination affects tumor aggressiveness remains unclear [2, 9]. Interestingly, levels of Glu-tubulin also increase following detachment and Glu-tubulin localizes within McTNs [2]. While microtubules composed of full-length α-tubulin have a half-life of minutes in cells, microtubules enriched in Glu-tubulin can persist for up to 16 h [10]. McTNs are additionally enriched with vimentin intermediate filaments (IF) [3]. The increased stability of Glu-microtubules is thought to result in part from the association with more resilient vimentin filaments [11, 12].

Members of the kinesin superfamily family (KIFs) function in chromosomal separation and spindle movements during mitosis and meiosis as well as trafficking materials in an anterograde direction along microtubules [13, 14]. Kinesin-1s or conventional kinesins consists of a tetramer made up of two heavy and two light chains. The globular N-terminal head domain of the heavy chain contains the highly conserved plus-end oriented motor domain and ATPase. The C-terminal end contains the stalk/tail region that interacts with cargo or with adaptor proteins [15]. In between the head and tail region lies the neck region that determines the directionality of the motor proteins [16]. Kinesins promote recruitment of IFs to Glu-tubulin [17] and cross-link these two filament systems [18]. The dependence of McTNs on coordinated vimentin and Glu-tubulin [2, 3] supports a possible role for kinesins in McTN formation.

The inhibitory effects of anesthetics on rapid axonal signaling have been well studied [19, 20]. In recent years, it was shown that local anesthetics inhibit kinesin motor function in an in vitro motility assay [21]. However, before the effects of Lidocaine and Tetracaine on kinesin proteins were known, it was discovered that Tetracaine possessed an inhibitory effect on metastatic mouse melanoma cells (B16-F1, B16-F10) that prevented successful reattachment of CTCs in distant tissues [1]. Tetracaine induced rounding of attached tumor cells and decreased cell-adhesion characteristics without affecting surface protein composition [1]. Despite the tremendous novelty of this finding, the specific mechanism underlying the anti-metastatic effect of anesthetics has not been pursued in more recent years and is still not completely understood.

The cytoskeletal mechanism supporting McTNs [2, 3] provides a potential connection between anesthetics, kinesins, and the reattachment process of CTCs. We, therefore, examined the effects of inhibiting kinesin activity on McTN motility and extension using the anesthetics Lidocaine and Tetracaine. We also investigated the effects of the anesthetics on vimentin filaments and on the motility of the conventional kinesin, kinesin-1, using a fluorescently tagged kinesin (GFP-Kif5c) within intact cells. Treatment with Tetracaine inhibited the extension of McTNs as well as their ability to promote tumor cell aggregation and reattachment. Lidocaine and Tetracaine caused rapid collapse of vimentin filaments within human MECs and breast tumor cells and live-cell video microscopy demonstrated that Tetracaine reduces motility of intracellular GFP-kinesin which causes centripetal collapse of McTNs. Our current data support a model where inhibition of kinesin motor proteins by Tetracaine leads to the reductions in McTNs and provides a novel mechanism for the ability of this anesthetic to reduce metastasis.

Materials and methods

Cell culture and drug treatment

MCF10A, a non-tumorigenic, immortalized MEC line, was cultured in 10 cm plastic dishes (Nunc/CellStar) with Dulbecco's modified Eagle's medium/F12 (DMEM) (Gibco) supplemented with 5% horse serum, insulin (5 μg/ml), EGF (20 ng/ml), hydrocortisone (500 ng/ml), penicillin–streptomycin (100 μg/ml each), and L-glutamine (2 mmol/l).

MCF10A-Bcl2 was grown in MCF10A media plus Puromycin (2 μg/ml) (Sigma). MDA-MB-436 and Hs578t cells were grown in DMEM with penicillin–streptomycin (100 μg/ml), L-glutamine (2 mmol/l), and 5% fetal bovine serum. Lidocaine hydrochloride monohydrate (Sigma) and Tetracaine hydrochloride (Sigma) were reconstituted in ddH_2O (0.5 M). Latrunculin-A (Biomol) was reconstituted in ethanol (5 mM). Treatments of MCF10A and MDA-MB-436 cells were with serum-free DMEM.

Immunofluorescence

MCF10A cells grown on glass coverslips were treated with DMEM or with DMEM plus the corresponding drug concentrations. Cells were fixed with methanol, blocked with 5% BSA/0.5% NP-40/PBS for 1 h before primary antibody incubation with ms-vimentin (1:1000; Zymed) in 2.5% BSA/0.5% NP-40-PBS for 1 h, anti-ms-Alexa Fluor-594, secondary antibody (1:500; Molecular Probe) for 1 h, ms-anti-α-Tubulin-FITC (1:500; Sigma), and Hoescht 33342 (1:5000; Sigma) for 1 h. All washes were done in PBS. Coverslips were mounted on glass slides using Fluoromount-G (SouthernBiotech, AL). Epifluorescent imaging was done on an Olympus IX-81 inverted microscope mounted with a CCD camera. Images were acquired using Volocity software (ImproVision Inc.; Waltham, MA).

For suspended IFs, MDA-MB-436s were detached using an enzyme-free cell dissociation solution (Millipore). Cells were suspended in phenol-red-free DMEM (Gibco) for 15 min, fixed in formaldehyde, and spun down over poly-lysine coated coverslips using a STATspin cytofuge (Iris Sampling Process, Inc.; Westwood, MA). Blocking, staining, and mounting were performed using similar methods as attached IF. Confocal images were acquired using an Olympus FV1000 laser scanning confocal microscope (Olympus, Center Valley, PA) equipped with a 60×/1.42 NA oil immersion objective lens with no zoom.

Westerns

MCF10A, MCF10A-Bcl2, and MDA-MB-436 cells were grown to confluency in 6-well dishes with or without the drugs Lidocaine, Tetracaine, or LA in DMEM. Cells were washed with PBS and gently scraped in ice-cold RIPA lysis buffer (50 mM Tris–HCl pH 8.0), 150 mM NaCl, 1% NP-40, 0.5% sodium deoxycholate, 0.1% SDS, 1 mM phenylmethylsulfonyl fluoride, and 1% protease inhibitor cocktail (Sigma,P2714)). To ensure total recovery, all media and washes were collected and pelleted by centrifugation for 5 min at 300×*g*. Pellets were lysed in RIPA Buffer and lysates combined. Lysates were incubated on ice for 15 min with vortexing before storage at -80°. Protein concentrations were measured using a Lowry-based assay (Bio-Rad, Hercules, CA). 20–30 μg of total protein was separated by SDS-PAGE on 12% polyacrylamide gels then transferred to Immuno-Blot PVDF membranes (Bio-Rad, Hercules, CA). Membranes were blocked in 5% milk in Tris-buffered saline (TBS) with 0.1% Tween for 1 h at room temperature followed by an overnight incubation at 4°C of each antibody separately, Rt-PARP (1:1000; H-250, Santa Cruz), Ms-Vimentin (1:1000; C-20, Santa Cruz), Ms-Bcl2 (1:1000, BD Transduction), and Ms-β-actin (1:1000: Sigma) in 2.5% milk TBS plus 0.1% Tween 20. Corresponding secondary antibodies to IgG conjugated to horseradish peroxidase (HRP) were used (1:5000; GE Healthcare, Piscataway, NJ) and visualized using ECL-plus chemiluminescent detection kit.

XTT viability assay

Cells were grown up to ~80% confluency in a clear bottomed 96 well plate (Costar; Corning, NY). Growth media were changed with 100 μl phenol-red-free DMEM media with or without Lidocaine or Tetracaine and incubated at 37°C. XTT salt solutions contained 1 mg/ml XTT salt (X-4626; Sigma) in phenol-free DMEM plus 7.7 ng/ml phenazine methosulfate (PMS). After incubation with 25 μl of XTT/PMS solution in each well (37°C, 4 h), absorbance at 450 nm was measured with a BioTek SynergyHT spectrophotometer.

Real-time cell attachment assay

Cell-substratum attachment was assessed by electrical impedance (xCelligence RTCA instrument, Roche). MCF10A, MCF10A-Bcl2, and MDA-MB-436 were trypsinized, counted, and diluted to a concentration of 10^6/ml. Duplicate wells of electronic microtiter E-plates were seeded with 10^5 cells in growth media containing 6 mM Lidocaine, 0.5 mM Tetracaine or. Raw cell index (CI) impedance values from each measured time point were normalized to the maximum CI attained for the parental control cell line at 1 h. Drug-treated cell lines were then represented as a percentage attachment related to untreated parental control.

Microtentacle scoring and live-cell imaging

MCF10A and/or MDA-MB-436 cells at ~50% confluency were transfected overnight with a vector expressing membrane-localized GFP (AcGFP1-Mem, ~1 μg/μl, Clontech, Mountain View, CA), using either Fugene6 transfection reagent (11814443001; Roche) or Exgen-500 (R0511; Fermentas). Cells were trypsinized, resuspended with DMEM or DMEM plus Lidocaine or Tetracaine ±5 μM Latrunculin A, transferred to a low-attachment plate, and incubated at

37°C for 15 min before counting. Live cells were blindly scored positive for McTNs when exhibiting two or more protrusions greater than the radius of the cell body. Populations of 100 or more GFP-positive cells were counted for each trial. Cell images were collected using an Olympus CKX41 inverted fluorescent microscope (Allentown, Pa) equipped with an Olympus F-View II 12-bit CCD digital camera system and Olympus MicroSuite5 imaging software. Movies of GFP-vimentin transfected cells were captured at 100× magnification and captured at one frame/2 s and are shown with a 5× acceleration. MCF10A and Hs578t cells at ~50% confluency were transfected with ~2 μg/μl of pGFP-KIF5C DNA, kindly provided by Dr. Michelle Peckham (Institute for Molecular and Cellular Biology, University of Leeds, Leeds, UK). Movies of GFP-kinesin transfected cells were captured at 100× magnification in a humidified 37°C chamber in a stack of 0.5 μm z-slices at approximately one frame/2–5 s using an Olympus IX81 inverted microscope. Analysis and particle tracking were done using the Volocity software (ImproVision Inc.; Waltham, MA).

Propidium iodide (PI) (Sigma; 1:3000, 20 min) staining was in phenol-red-free DMEM and trypsinized cells were scored blindly positive for PI on an Olympus CKX41 inverted fluorescent microscope.

Results

Inhibition of microtentacles by the local anesthetics Lidocaine and Tetracaine

To visualize McTNs, MCF10A, and MDA-MB-436 cells were transfected with a membrane-localizing green

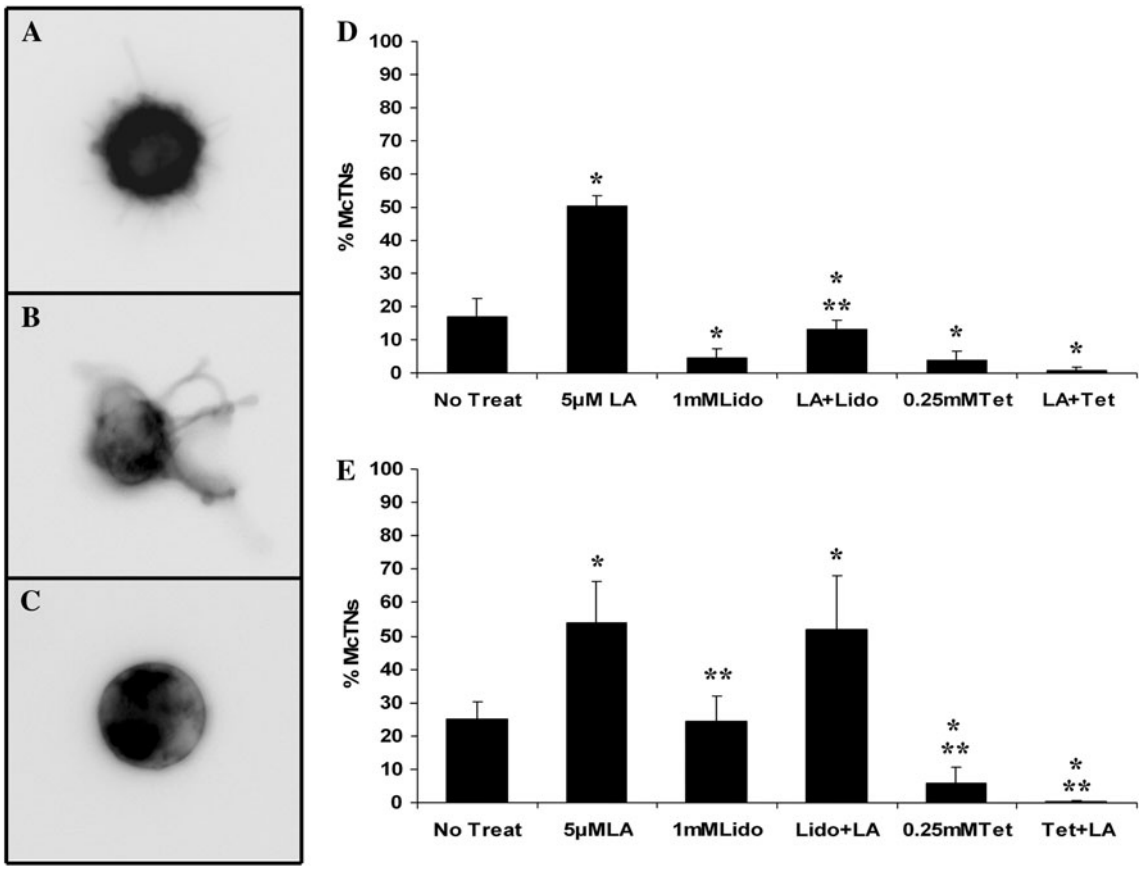

Fig. 1 Tetracaine is an effective inhibitor of McTN protrusions in MCF10A and MDA-MB-436 cells. MCF10A human mammary epithelial cells and MDA-MB-436 human breast cancer cells were transfected with GFP-Membrane and scored for microtentacle (McTN) generation. **a–c** Representation of McTN types counted and not counted, **a** DMEM (positive), **b** 5 μM LA (positive), **c** 0.25 mM Tetracaine + LA (negative), **d** MCF10A $n = 4$, **e** MDA-MB-436 $n = 4$ McTN counts, **d**, **e** MCF10A and MDA-MB-436 cells either under No Treatment, 5 μM LA, 1 mM Lidocaine ± 5μMLA, or 0.25 mM Tetracaine ± 5μMLA. Cells were blindly scored positive when exhibiting two or more McTNs that extended greater than the radius of the cell body. Three independent experiments with at least 100 GFP-positive cells were counted for each bar. In MCF10A cells, 1 mM Lidocaine and 0.25 mM Tetracaine were effective in inhibiting McTN ± LA. In MDA-MB-436 cells, only 0.25 mM Tetracaine was effective in inhibiting McTNs ± LA but not effective in 1 mM Lidocaine. * indicates significant difference compared to that of No Treatment. ** indicates significant difference compared to that of 5 μM LA treatment. Statistical analyses were done with an ANOVA test, $P < 0.05$

fluorescent protein (GFP-Mem) [2, 3] and suspended over low-attachment plates before blindly scoring for McTNs that extend longer than the radius of the cells (Fig. 1a–c). Latrunculin-A, an actin depolymerizer, increased the length and frequency of McTNs in MCF10A and MDA-MB-436 cells (Fig. 1d, e), as did another actin depolymerizer, Cytochalasin-D (not shown) [22, 23]. In MCF10A cells, Lidocaine and Tetracaine reduced McTNs; however, in MDA-MB-436 cells, 1 mM Lidocaine did not significantly reduce McTNs. It is possible that MDA-MB-436 cells possess a greater resistance to Lidocaine due to the large quantity of vimentin filaments that may confer additional stabilization (Fig. 2c). Tetracaine, however, a more potent inhibitor of kinesins, reduced McTN frequencies for both cell lines, even in the presence of the actin depolymerizers Cytochalasin-D (not shown) and LA (Fig. 1d, e) [21].

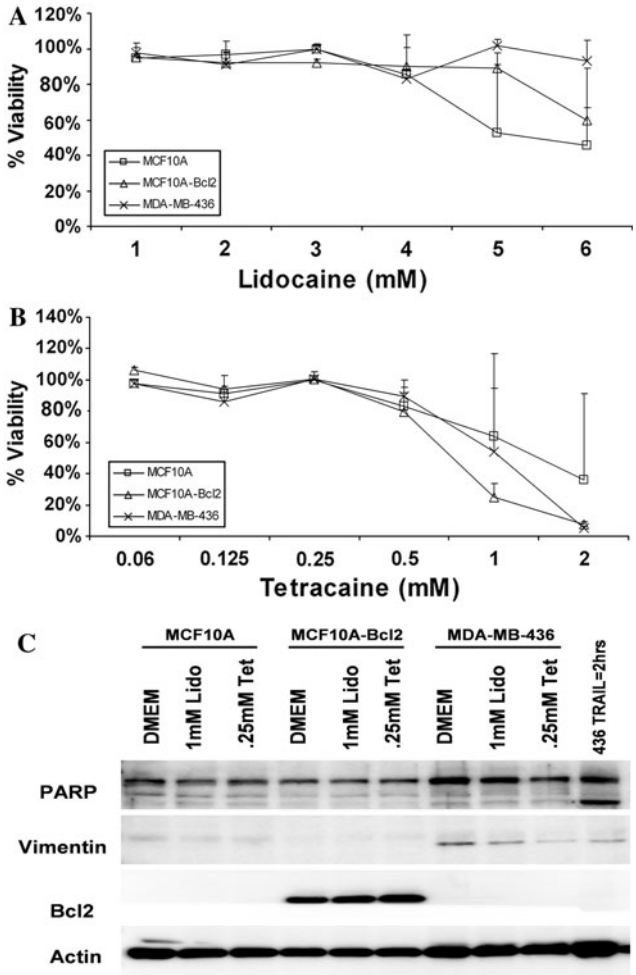

Fig. 2 Lidocaine and Tetracaine do not affect cellular viability or induce PARP at the concentrations that inhibit microtentacle protrusions. **a**, **b** XTT Viability Assay on MCF10A, MCF10A-Bcl2, and MDA-MB-436 cells in a 96-well plate for 4 h. Cells are viable after 4 h of treatment at the concentrations 1 mM Lidocaine and 0.25 mM Tetracaine ($n = 3$, each trial done in triplicate). **c** Western Blot: MCF10A, MCF10A-Bcl2, and MDA-MB-436 samples with/without Lidocaine and Tetracaine treatments were run on 12% polyacrylamide gels and blotted for PARP cleavage, Vimentin, Bcl2, and actin. MDA-MB-436 was additionally treated with 1 μg/ml TRAIL for 2 h as a positive control for cleaved PARP. Lidocaine and Tetracaine do not cause significant PARP cleavage in the three cell lines tested at the working concentrations of 1 mM Lidocaine and 0.25 mM Tetracaine after 4 h of treatment

Concentrations of Lidocaine and Tetracaine that inhibit microtentacles are non-toxic to human mammary epithelial cells and breast tumor cell lines

The effects of Lidocaine and Tetracaine on the viability of human MECs have not been well-established, but tetrazolium hydroxide viability assays confirmed that these anesthetics are non-toxic above and below the concentrations used for McTN inhibition. While McTNs are affected after 15 min of treatment with either 1 mM Lidocaine or 0.25 mM Tetracaine, no toxicity is observed at these concentrations for human MECs (MCF10A, MCF10A-Bcl2) and a human breast tumor cell line (MDA-MB-436) even after 4 h of exposure (Fig. 2a, b). Extended treatments for 24 h with 1 mM Lidocaine or 0.25 mM Tetracaine reduced MCF10A viability compared to that of MCF10A-Bcl2 and MDA-MB-436s (not shown). However, as MCF10A cells are highly sensitive to apoptotic cell death, particularly in response to changes in cell shape [24], the resistance conferred by Bcl-2 expression showed that anesthetics were not toxic to apoptotically resistant cells. To determine if treatments with anesthetics would induce short-term apoptosis in MCF10A cells, a western blot was performed to assay cleavage of Poly-(ADP-ribose)-polymerase (PARP) (Fig. 2c). Treatment with the anesthetics did not induce PARP cleavage at 4 h, even though apoptosis is functionally active as shown by a positive control treatment with tumor necrosis (TNF)-related apoptosis-inducing ligand (TRAIL). A propidium iodide exclusion assay further confirmed that membrane integrity was maintained in MCF10A and MDA-MB-436 cells under the same drug conditions utilized for McTN counts (Supplemental Data 1).

Lidocaine and Tetracaine cause a centripetal collapse of vimentin intermediate filaments and inhibit vimentin trafficking

The effects of Lidocaine and Tetracaine on the cytoskeleton structural components, α-tubulin and vimentin, were analyzed via immunofluorescence of MCF10A (Fig. 3a) and MDA-MB-436 (Fig. 3b) cells. Long filaments of α-tubulin proteins (Fig. 3a1, b1) and vimentin IFs (Fig. 3a2, b2) were found ubiquitously throughout the cytoplasm before treatment with inhibitors. After 30 min of incubation in 1 mM Lidocaine or 0.25 mM Tetracaine, vimentin

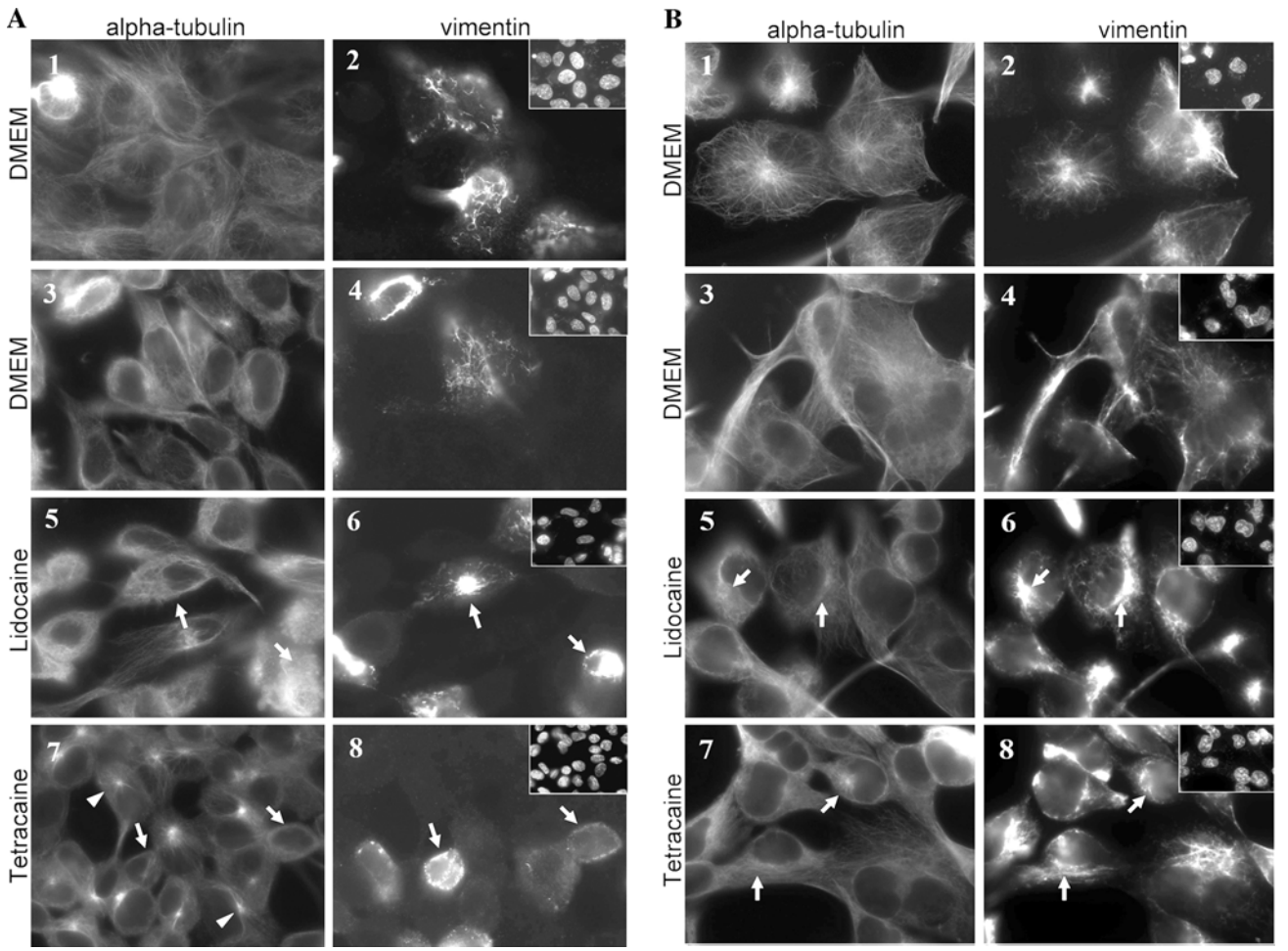

Fig. 3 Anesthetic treatment causes collapse of vimentin intermediate filaments MCF10A cells (**a**) and MDA-MB-436 cells (**b**) were fixed and immunostained for α-tubulin and vimentin. *1*, *2* $T = 0$ in DMEM *3*, *4* $T = 30$ min in DMEM *5*, *6* DMEM + 1 mM Lidocaine *7*, *8* DMEM + 0.25 mM Tetracaine. *Arrows* point to areas of vimentin collapse at $T = 30$ min with 1 mM Lidocaine and 0.25 mM Tetracaine treatment with corresponding arrows in α-tubulin. Vimentin collapse occurs in both MCF10A and MDA-MB-436 cells at $T = 30$ min in both 1 mM Lidocaine and 0.25 mM Tetracaine treatment. *Arrowheads* (**a** *7*) point to focal points of α-tubulin collapse seen in MCF10A cells. Hoescht DNA stain in top, right insets

filaments in MCF10A and MDA-MB-436 cells collapse to a perinuclear position (Fig. 3a6, 8; b6, 8), consistent with the vimentin collapse observed in fibroblasts when the anterograde movement of kinesins is inhibited [25, 26]. However, microtubules remained filamentous with no differences between treatments and DMEM control (Fig. 3a5, 7; b5, 7), although intriguing foci of α–tubulin can be seen in MCF10A cells at 30 min (Figs. 3a, 7 white arrowhead).

We further investigated the effects of Tetracaine on the vimentin and α-tubulin networks of suspended MDA-MB-436s (Fig. 4). Control cells displayed McTNs composed of filamentous vimentin and α-tubulin [3]. Cells treated with 0.25 mM Tetracaine, however; displayed a marked decrease in vimentin containing McTNs.

To examine Lidocaine and Tetracaine's inhibitory effect on vimentin trafficking along microtubules, live-cell fluorescence video microscopy was performed in MCF10A cells expressing GFP-vimentin. Kinesin motor proteins traffic vimentin monomers and squiggles in an anterograde direction toward microtubule plus-ends [26]. GFP-vimentin moved similarly as circular, wobble, and linear particles that were inhibited by treatment with Lidocaine or Tetracaine. Cessation of GFP-vimentin motion occurred at approximately 4 min with Tetracaine and approximately 10 min with Lidocaine (Supplemental Data 2).

Local anesthetics attenuate reattachment of suspended mammary epithelial cells and breast tumor cell lines

Tetracaine modifies microfilament organization and decreases cell adhesion characteristics in endothelial and subendothelial cell adhesion assays [1]. To assess the effect

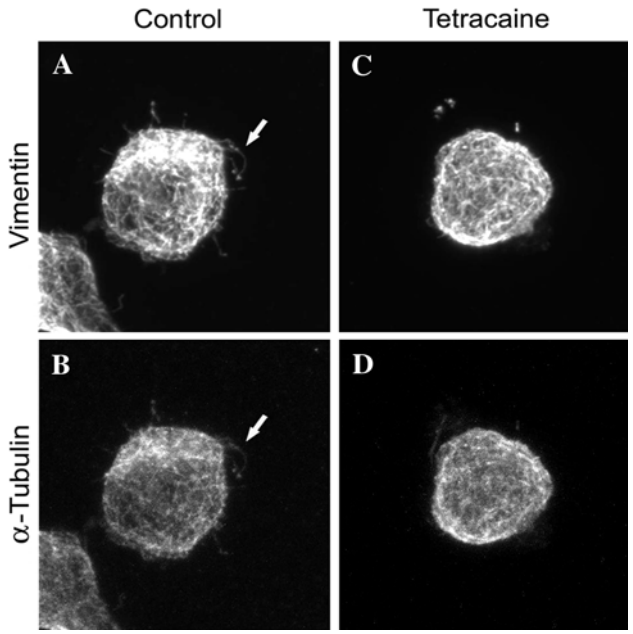

Fig. 4 Anesthetic treatment of suspended MDA-MB-436 cells cause the collapse of vimentin and α-tubulin suspended MDA-MD-436 cells were left untreated (**a**, **b**) or treated with 0.25 mM Tetracaine (**c**, **d**) fixed and immunostained for vimentin (**a**, **c**) or α-tubulin (**b**, **d**) after 15 min of suspension. *Arrows* point to microtentacles with vimentin and α-tubulin staining in the control cells (**a**, **b**). Suspended cells treated with Tetracaine show decreased vimentin extension and microtentacle protrusions (**c**, **d**)

of Tetracaine and Lidocaine on cell-substratum adhesion properties of MCF10A, MCF10A-Bcl2, and MDA-MB-436 cell lines, the xCelligence RTCA SP real-time cell sensing system was used to measure dynamic cell reattachment. Lidocaine concentrations were increased from 1 to 3 mM after preliminary studies determined improved inhibition of reattachment. In all cell lines, reattachment was greatly attenuated with drug treatments up to 2 h. While MCF10A-Bcl2 cells attach more quickly than MCF10A cells between 90 and 140 min, they are still inhibited by Lidocaine and Tetracaine (Fig. 5b). Overall, reattachment of both MCF10A MECs and MDA-MB-436 breast tumor cells were significantly ($P < 0.05$, *t*-test) inhibited by anesthetic treatment (Fig. 5a–c).

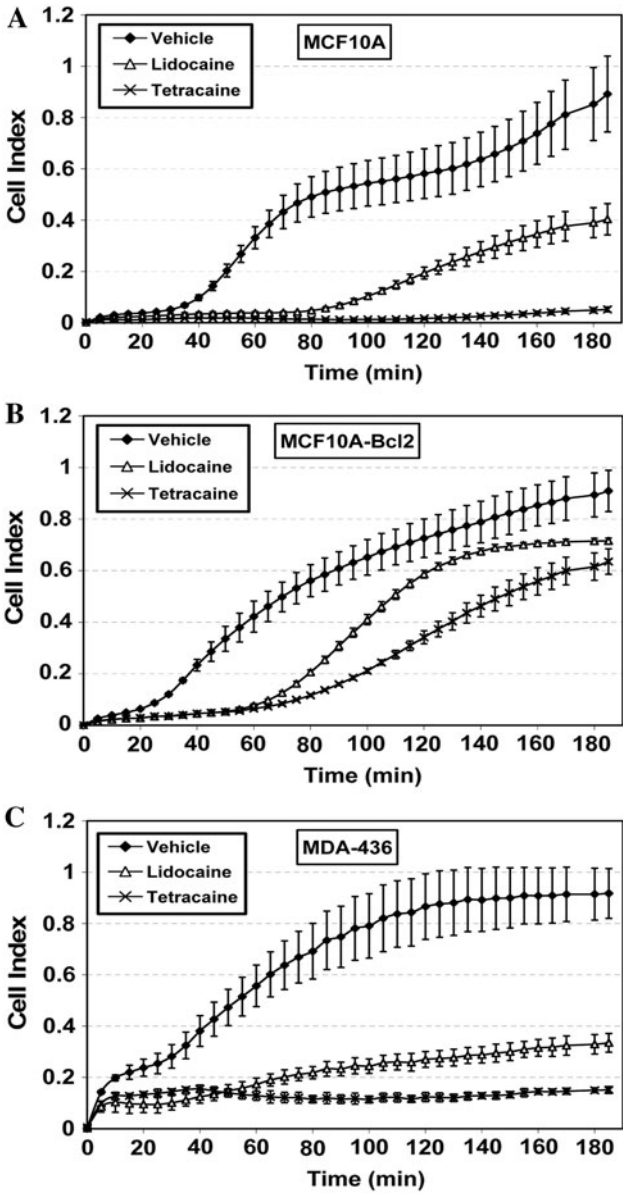

Fig. 5 Lidocaine and Tetracaine impede reattachment of human MECs. MCF10A (**a**), MCF10A-Bcl2 (**b**), and MDA-MB-436 breast tumor cells (**c**). Attachment was measured through impedance of electrical current using the xCelligence RTCA SP real-time cell sensing instrument in the presence of Lidocaine (1 mM) or Tetracaine (0.25 mM) as indicated

Tetracaine causes the rapid centripetal collapse of microtentacles

To directly observe the effects of Tetracaine on McTNs, live-cell microscopy was performed to image McTN dynamics during drug treatment. MDA-MB-436 cells were imaged over glass coverslips coated with bovine serum albumin to reduce reattachment. In the DMEM vehicle control, dynamic McTN motion persisted for extended periods of time (Fig. 6, Supplementary Data 3). Upon addition of 125 μM Tetracaine, a rapid reduction in McTN length and frequency was observed, accompanying a complete retraction of all protrusions by 12 min similar to the observations made with compounds targeting vimentin assembly in McTNs [3].

Additional studies were done on the rate of homotypic aggregation in suspended populations of MCF10A, MCF10A-Bcl2, and MDA-MB-436 cells in the presence of Lidocaine or Tetracaine. Cells were suspended in 0.2% methylcellulose media and an image was generated for

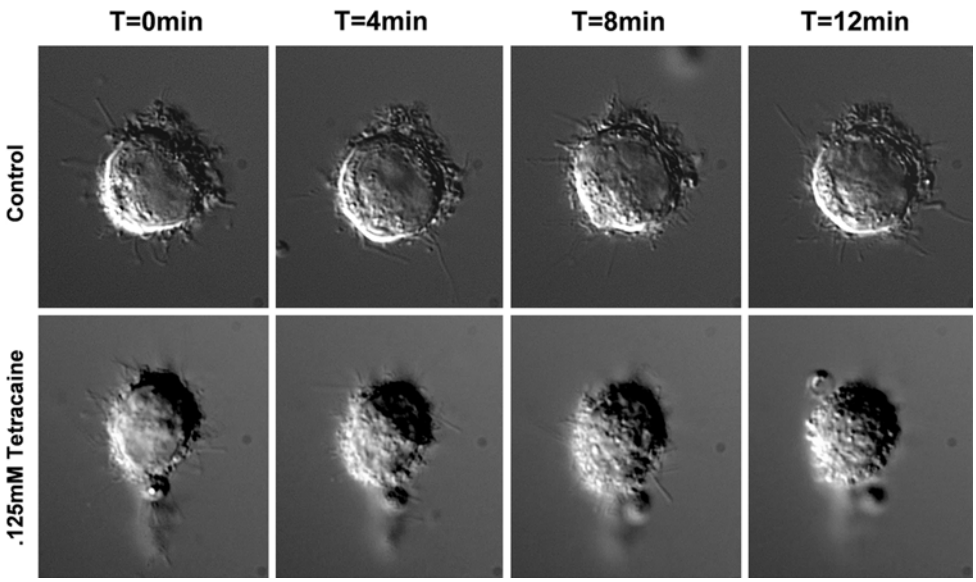

Fig. 6 Tetracaine causes the reabsorption of microtentacle protrusions. Still, time-lapse images of suspended MDA-MD-436 cells in Phenol-red-free DMEM. Cells have been allowed to partially attach to the bottom of a glass culture dish and filmed using DIC microscopy. In control cells, microtentacles persist up to 12 min but when treated with 0.125 mM Tetracaine, microtentacles collapse and are reabsorbed completely by 12 min. Time-lapse movies in supplemental data

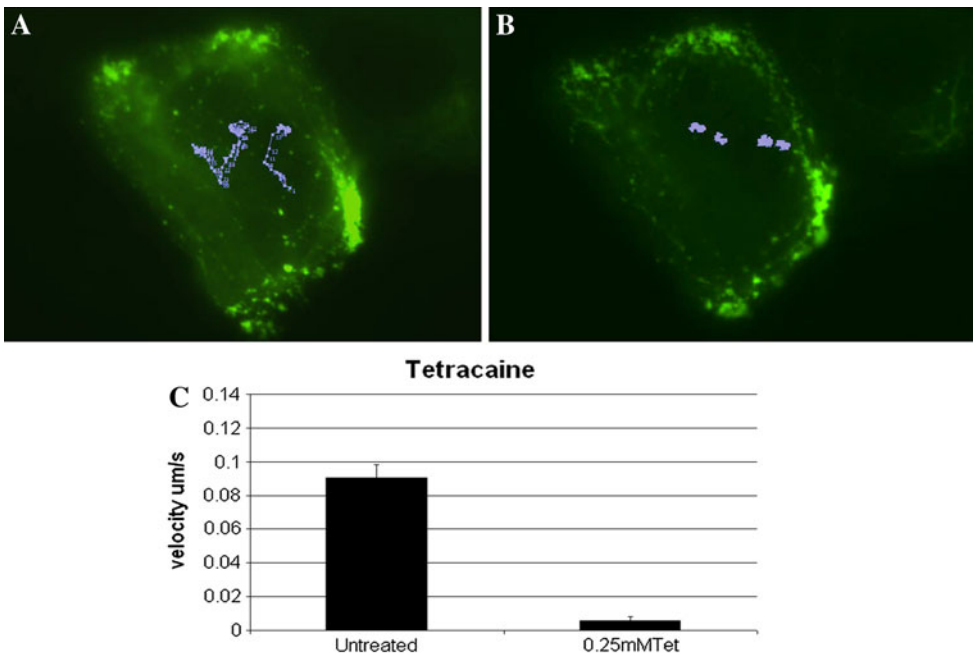

Fig. 7 GFP-KIF5C forward motion is inhibited by Tetracaine. MCF10A human MECs were transfected with a GFP-tagged full-length kinesin-1 motor protein, GFP-KIF5C. GFP-KIF5C movements were observed using live-cell microscopy within MCF10A cells before treatment (**a**) and after treatment with Tetracaine (**b**) where velocities of selected GFP speckles were observed and tracked. Significant differences in velocities are observed ($n = 3$, $P < 0.05$, t-test) (**c**)

every 15 min. Aggregation was observed 30–60 min after suspension in all cell lines with the greatest inhibition of aggregation in Tetracaine-treated cells compared to that of DMEM control wells while Lidocaine did not significantly reduce the aggregation rate (Supplementary Data 4).

Tetracaine inhibits intracellular kinesin motor motility

To specifically examine the effect of Tetracaine on kinesins, MCF10A cells were transfected with GFP-KIF5C, a kinesin-1-GFP fusion protein, and analyzed for small GFP-particle movements and trafficking [27]. As shown by Peckham and colleagues [27], GFP-KIF5C particles were visualized in MCF10A cells as speckles moving along microtubules at varying velocities with intermittent movements. To observe the impact of anesthetic on kinesin motility, time-lapse movies were taken before and after treatment with Tetracaine. Clear, motile GFP particles were tracked and recorded at 5 frames/min for vehicle control and drug treatment starting at 4 min after treatment.

Cells treated with DMEM control moved deliberately along tracks. Cells treated with Tetracaine displayed particles that can be seen slowing with almost complete inhibition of movement between 4 to 10 min after treatment (Fig. 7a–c, Supplementary Data 5).

Discussion

Attached cells establish and maintain their morphology via the counterbalance of microtubule extension from the microtubule-organizing center and the contractile forces generated by the actin cytoskeleton [28, 29]. When a cell becomes detached, cell death is induced by the disruption of this balance and cell survival becomes dependent on (1) reattachment to a surface or (2) apoptotic insensitivity [8, 24]. Given the harsh environment of the bloodstream for most solid tumor cells, the ability of metastatic cells to reattach is essential for tumor cell survival. We have proposed that suspended cells actively facilitate the reattachment process by extending McTNs that are enriched in coordinated Glu-tubulin and vimentin intermediate filaments [2, 3]. Supporting evidence shows that the frequency and length of the McTNs increase in highly metastatic tumor lines [3]. This suggests an adaptation that improves the survival of detached tumor cells through increased efficiency of reattachment. Glu-tubulin and vimentin levels both correlate with the metastatic potential, invasiveness, and McTN frequency in breast cancer cells [2, 9, 30]. In addition, direct microtubule stabilization by the tubulin-binding protein, Tau, increases the metastatic efficiency of circulating tumor cells and tumor cell reattachment by promoting McTN formation [31].

Growing evidence indicates that microtubule modifications contribute to the regulation of kinesin motor proteins with preferential binding of specific kinesins to distinct subpopulations [32, 18]. Kinesins also regulate interactions between microtubules and vimentin filaments and thus may play a direct role in cross-linking Glu-tubulin and vimentin filaments [17, 18]. Inhibition of kinesins destabilizes tubulin–vimentin cross-linking and collapses vimentin filaments (Fig. 3) [25, 26]. In attached cells, kinesins move along microtubule tracks to deliver components required for the regulation of focal adhesions at the microtubule caps [33]. It is likely that kinesins play a similar role in McTNs by recruiting supportive structures such as vimentin and MAPs to regulate McTN length and growth. In addition, by inhibiting kinesin anterograde movement, the remaining retrograde movement of dynein motor proteins along microtubules may initiate the disassembly of vimentin filaments and cause the re-absorption of McTNs. The Glu-tubulin–vimentin association may also become destabilized by the decreased availability of vimentin components required for the extension of IFs and McTNs (Fig. 3). The resulting catastrophe at the microtubule plus-ends could cause the retraction of McTNs and reduce the rate of cell reattachment.

Lidocaine and Tetracaine are commonly known local anesthetics that inhibit kinesin motor protein function in in vitro motility assays [21, 34]. This inhibitory activity was linked to the ability of Lidocaine and Tetracaine to prevent the forward motion of kinesins along microtubules, without affecting the capacity to bind microtubules, ATP, or cargo proteins [21]. We tested the hypothesis that inhibiting the motility of kinesin motor proteins would reduce McTN extension by preventing transport of the required components for McTNs. In live-cell counts of suspended MCF10A and MCF10A-Bcl2 cells, application of Lidocaine and Tetracaine significantly reduced McTN counts. However, Lidocaine had no significant effect on MDA-MB-436 cells (Fig. 1), which may result from the abundance of vimentin within the cells. In vitro studies postulate the inhibition of kinesin motility by Lidocaine and Tetracaine is due to the interactions of the charged form of the inhibitors with the neck region of the kinesin motor proteins, which unwinds to allow the forward stepping process to occur and thus the rotation of the microtubule-free head after ATP hydrolysis [18 ,35, 36]. Lidocaine and Tetracaine were not found to compete for kinesin binding to microtubules or impede ATP hydrolysis, but instead uncoupled ATP hydrolysis from kinesin movement [21]. Live-cell video microscopy demonstrated the rapid reabsorption of McTNs in MDA-MB-436 cells after Tetracaine application (Fig. 6, Supplementary Data 3). Additional live-cell movies of transiently transfected GFP-KIF5C in MCF10A cells confirmed a direct effect of Tetracaine inhibition on kinesin movement within intact cells (Fig. 7, Supplementary Data 5, 6). CTCs reattach to blood vessel walls in distant tissues via a mechanism consistent with the formation of McTNs. Breast tumor cells are generally too large to fit through capillaries, causing efficient trapping and fragmentation of CTCs in the first capillary bed encountered after entering the bloodstream [37, 38]. The ability of breast tumor cells to successfully adhere to blood vessel walls and escape the circulation is, therefore, an important determinant of metastatic efficiency. In a study by Nicolson et al., B16 melanoma cells pretreated with Tetracaine were injected into syngeneic C57BL/6 mice [1]. Tetracaine-treated cells displayed a decreased retention in lung capillaries by 2–5-fold while overall metastasis was also decreased compared to the control [1]. It was proposed that Tetracaine's effects on cell morphology, agglutination, receptor distribution, and adherence explained the decrease in lung tumor colonies; however, the underlying mechanisms were never clarified [1]. The coordination of cytoskeletal filaments underlying McTNs provides a target to

bring together these compelling in vivo studies with the more recent in vitro observations that anesthetics reduce kinesin motility. Our data show that Tetracaine inhibits kinesin motility within intact cells and induces collapse of the vimentin filaments that support McTNs. This provides a novel molecular mechanism for the action of Tetracaine to reduce the metastatic efficiency of CTCs.

Acknowledgments This work was supported by 1R01CA124704-01 from the National Cancer Institute (to S.S.M.), a Breast Cancer Idea Award (BC061047) from the USA Medical Research and Materiel Command (to S.S.M.) and a Clinical Innovator award from the Flight Attendant Medical Research Institute (FAMRI, CIA-062497).

Conflicts of interest The authors declare no conflicts of interest.

References

1. Nicolson GL, Fidler IJ, Poste G (1986) Effects of tertiary amine local anesthetics on the blood-borne implantation and cell surface properties of metastatic mouse melanoma cells. J Natl Cancer Inst 76:511–519
2. Whipple RA, Cheung AM, Martin SS (2007) Detyrosinated microtubule protrusions in suspended mammary epithelial cells promote reattachment. Exp Cell Res 313:1326–1336
3. Whipple RA, Balzer EM, Cho EH, Matrone MA, Yoon JR, Martin SS (2008) Vimentin filaments support extension of tubulin-based microtentacles in detached breast tumor cells. Cancer Res 68:5678–5688
4. Korb T, Schluter K, Enns A, Spiegel HU, Senninger N, Nicolson GL, Haier J (2004) Integrity of actin fibers and microtubules influences metastatic tumor cell adhesion. Exp Cell Res 299:236–247
5. Machesky LM (2008) Lamellipodia and filopodia in metastasis and invasion. FEBS Lett 582(14):2102–2111
6. Donaldson DJ, Dunlap MK (1981) Epidermal cell migration during attempted closure of skin wounds in the adult newt: observations based on cytochalasin treatment and scanning electron microscopy. J Exp Zool 217:33–43
7. Frisch SM, Francis H (1994) Disruption of epithelial cell-matrix interactions induces apoptosis. J Cell Biol 124:619–626
8. Reed JC (1998) Dysregulation of apoptosis in cancer. Cancer J Sci Am 4(Suppl 1):S8–S14
9. Mialhe A, Lafanechere L, Treilleux I, Peloux N, Dumontet C, Bremond A, Panh MH, Payan R, Wehland J, Margolis RL, Job D (2001) Tubulin detyrosination is a frequent occurrence in breast cancers of poor prognosis. Cancer Res 61:5024–5027
10. Webster DR, Gundersen GG, Bulinski JC, Borisy GG (1987) Assembly and turnover of detyrosinated tubulin in vivo. J Cell Biol 105:265–276
11. Janmey PA, Euteneuer U, Traub P, Schliwa M (1991) Viscoelastic properties of vimentin compared with other filamentous biopolymer networks. J Cell Biol 113:155–160
12. Gurland G, Gundersen GG (1995) Stable, detyrosinated microtubules function to localize vimentin intermediate filaments in fibroblasts. J Cell Biol 131:1275–1290
13. Sharp DJ, Rogers GC, Scholey JM (2000) Microtubule motors in mitosis. Nature 407:41–47
14. Vale RD, Reese TS, Sheetz MP (1985) Identification of a novel force-generating protein, kinesin, involved in microtubule-based motility. Cell 42:39–50
15. Coy DL, Hancock WO, Wagenbach M, Howard J (1999) Kinesin's tail domain is an inhibitory regulator of the motor domain. Nat Cell Biol 1:288–292
16. Endow SA, Waligora KW (1998) Determinants of kinesin motor polarity. Science 281:1200–1202
17. Kreitzer G, Liao G, Gundersen GG (1999) Detyrosination of tubulin regulates the interaction of intermediate filaments with microtubules in vivo via a kinesin-dependent mechanism. Mol Biol Cell 10:1105–1118
18. Liao G, Gundersen GG (1998) Kinesin is a candidate for cross-bridging microtubules and intermediate filaments. Selective binding of kinesin to detyrosinated tubulin and vimentin. J Biol Chem 273:9797–9803
19. Fink BR, Kennedy RD, Hendrickson AE, Middaugh ME (1972) Lidocaine inhibition of rapid axonal transport. Anesthesiology 36:422–432
20. Richards CD (1978) The action of anaesthetics on synaptic transmission. Gen Pharmacol 9:287–293
21. Miyamoto Y, Muto E, Mashimo T, Iwane AH, Yoshiya I, Yanagida T (2000) Direct inhibition of microtubule-based kinesin motility by local anesthetics. Biophys J 78:940–949
22. Spector I, Shochet NR, Kashman Y, Groweiss A (1983) Latrunculins: novel marine toxins that disrupt microfilament organization in cultured cells. Science 219:493–495
23. Casella JF, Flanagan MD, Lin S (1981) Cytochalasin D inhibits actin polymerization and induces depolymerization of actin filaments formed during platelet shape change. Nature 293: 302–305
24. Martin SS, Leder P (2001) Human MCF10A mammary epithelial cells undergo apoptosis following actin depolymerization that is independent of attachment and rescued by Bcl-2. Mol Cell Biol 21:6529–6536
25. Gyoeva FK, Gelfand VI (1991) Coalignment of vimentin intermediate filaments with microtubules depends on kinesin. Nature 353:445–448
26. Prahlad V, Yoon M, Moir RD, Vale RD, Goldman RD (1998) Rapid movements of vimentin on microtubule tracks: kinesin-dependent assembly of intermediate filament networks. J Cell Biol 143:159–170
27. Dunn S, Morrison EE, Liverpool TB, Molina-Paris C, Cross RA, Alonso MC, Peckham M (2008) Differential trafficking of Kif5c on tyrosinated and detyrosinated microtubules in live cells. J Cell Sci 121:1085–1095
28. Ingber DE (2002) Mechanical signaling and the cellular response to extracellular matrix in angiogenesis and cardiovascular physiology. Circ Res 91:877–887
29. Ingber DE (2003) Tensegrity II. How structural networks influence cellular information processing networks. J Cell Sci 116: 1397–1408
30. Blick T, Widodo E, Hugo H, Waltham M, Lenburg ME, Neve RM, Thompson EW (2008) Epithelial mesenchymal transition traits in human breast cancer cell lines. Clin Exp Metastasis 25:629–642
31. Matrone MA, Whipple RA, Thompson K, Cho EH, Vitolo MI, Balzer EM, Yoon JR, Ioffe OB, Tuttle KC, Tan M, Martin SS (2010) Metastatic breast tumors express increased tau, which promotes microtentacle formation and the reattachment of detached breast tumor cells. Oncogene 1–11
32. Hammond JW, Huang CF, Kaech S, Jacobson C, Banker G, Verhey KJ (2010) Posttranslational modifications of tubulin and the polarized transport of kinesin-1 in neurons. Mol Biol Cell 21:572–583
33. Krylyshkina O, Kaverina I, Kranewitter W, Steffen W, Alonso MC, Cross RA, Small JV (2002) Modulation of substrate adhesion dynamics via microtubule targeting requires kinesin-1. J Cell Biol 156:349–359

34. Tsuda Y, Mashimo T, Yoshiya I, Kaseda K, Harada Y, Yanagida T (1996) Direct inhibition of the actomyosin motility by local anesthetics in vitro. Biophys J 71:2733–2741
35. Crevel IM, Lockhart A, Cross RA (1996) Weak and strong states of kinesin and ncd. J Mol Biol 257:66–76
36. Hirose K, Lockhart A, Cross RA, Amos LA (1995) Nucleotide-dependent angular change in kinesin motor domain bound to tubulin. Nature 376:277–279
37. Morris VL, MacDonald IC, Koop S, Schmidt EE, Chambers AF, Groom AC (1993) Early interactions of cancer cells with the microvasculature in mouse liver and muscle during hematogenous metastasis: videomicroscopic analysis. Clin Exp Metastasis 11:377–390
38. Tsuji K, Yamauchi K, Yang M, Jiang P, Bouvet M, Endo H, Kanai Y, Yamashita K, Moossa AR, Hoffman RM (2006) Dual-color imaging of nuclear-cytoplasmic dynamics, viability, and proliferation of cancer cells in the portal vein area. Cancer Res 66:303–306